Hyperactivation of the Frontal Control Network Revealed by Symptom Provocation in Obsessive-Compulsive Disorder Using EEG Microstate and sLORETA Analyses

Yoshimura, Masafumi ; Pascual-Marqui, Roberto D ; Nishida, Keiichiro ; Kitaura, Yuichi ; Mii, Hiroshi ; Saito, Yukiko ; Ikeda, Shunichiro ; Katsura, Koji ; Ueda, Satsuki ; Minami, Shota ; Isotani, Toshiaki ; Kinoshita, Toshihiko

Abstract: The aim of this study was to investigate the changes of brain electric field induced by symptom provocation in patients with obsessive-compulsive disorder (OCD) in comparison to healthy controls in the resting state. For this purpose, EEG recordings in conditions of initial rest, clean control, symptom provocation by imaginal exposure, and final rest were used for computing spatiotemporal activity characteristics based on microstate segmentation. Within-group comparisons were significant for the symptom provocation condition: OCD showed high global field power (GFP) and transition rates into a medial frontal microstate, whereas healthy controls showed high frequency of occurrence and high percent of dwelling time for a medial occipitoparietal microstate. Between-group comparisons demonstrated significantly lower GFP and dwelling time for the medial occipitoparietal microstate in OCD in several conditions including initial rest and symptom provocation. In addition, OCD compared to healthy controls showed significant instability of the medial occipitoparietal microstate, with high preference for transitions into the medial frontal microstate. In conclusion, during rest and symptom provocation, OCD patients make preferential use of a medial frontal brain network, with concomitant reduction of use of a medial occipitoparietal network, as shown by dwelling times, explained variance, and dynamic transition rates. These findings support the idea of a possible biological marker for OCD, which might correspond to pathological hyperactivation of the frontal control network.

DOI: https://doi.org/10.1159/000491719

Original Paper

Neuropsychobiology

Neuropsychobiology
DOI: 10.1159/000491719

Received: March 12, 2018
Accepted after revision: June 28, 2018
Published online: September 24, 2018

Hyperactivation of the Frontal Control Network Revealed by Symptom Provocation in Obsessive-Compulsive Disorder Using EEG Microstate and sLORETA Analyses

Masafumi Yoshimura[a] Roberto D. Pascual-Marqui[a, b] Keiichiro Nishida[a] Yuichi Kitaura[a] Hiroshi Mii[a, c] Yukiko Saito[a] Shunichiro Ikeda[a, d] Koji Katsura[a] Satsuki Ueda[a] Shota Minami[a] Toshiaki Isotani[a, e] Toshihiko Kinoshita[a]

[a]Department of Neuropsychiatry, Kansai Medical University, Osaka, Japan; [b]The KEY Institute for Brain-Mind Research, University Hospital of Psychiatry, Zurich, Switzerland; [c]Setagawa Hospital, Otsu, Japan; [d]Department of Psychiatric Neurophysiology, University Hospital of Psychiatry, Bern, Switzerland; [e]Department of Brain-Mind Research, Shikoku University Faculty of Nursing, Tokushima, Japan

Keywords
Electroencephalographic microstates · Electroencephalography · Obsessive-compulsive disorder · Standardized low-resolution electromagnetic tomography, symptom provocation

Abstract
The aim of this study was to investigate the changes of brain electric field induced by symptom provocation in patients with obsessive-compulsive disorder (OCD) in comparison to healthy controls in the resting state. For this purpose, EEG recordings in conditions of initial rest, clean control, symptom provocation by imaginal exposure, and final rest were used for computing spatiotemporal activity characteristics based on microstate segmentation. Within-group comparisons were significant for the symptom provocation condition: OCD showed high global field power (GFP) and transition rates into a medial frontal microstate, whereas healthy controls showed high frequency of occurrence and high percent of dwelling time for a medial occipitoparietal microstate. Between-group comparisons demonstrated significantly lower GFP and dwelling time for the medial occipitoparietal microstate in OCD in several conditions including initial rest and symptom provocation. In addition, OCD compared to healthy controls showed significant instability of the medial occipitoparietal microstate, with high preference for transitions into the medial frontal microstate. In conclusion, during rest and symptom provocation, OCD patients make preferential use of a medial frontal brain network, with concomitant reduction of use of a medial occipitoparietal network, as shown by dwelling times, explained variance, and dynamic transition rates. These findings support the idea of a possible biological marker for OCD, which might correspond to pathological hyperactivation of the frontal control network.

KARGER

E-Mail karger@karger.com
www.karger.com/nps

Masafumi Yoshimura
Department of Neuropsychiatry, Kansai Medical University
10–15 Fumizono-cho
Moriguchi, Osaka 5708507 (Japan)
E-Mail yoshimum@takii.kmu.ac.jp

Introduction

Obsessive-compulsive disorder (OCD) is defined in DSM-5 [1] by the presence of obsessions and/or compulsions. Obsessions are repetitive and persistent thoughts, urges, or images that are experienced as intrusive and unwanted, whereas compulsions are recurrent behaviors or mental acts that an individual feels driven to perform in response to an obsession or according to rules that must be applied rigidly. Lifetime prevalence has been estimated to be about 2–3% [2].

Recent systematic research, mainly performed by neuroimaging strategies, has demonstrated that OCD is associated with dysfunction of the corticostriatothalamocortical circuitry, particularly in the orbitofrontal cortex and caudate nucleus [3]. Electrophysiological studies [4] investigated the cortical source localization in 50 OCD patients in comparison with 50 normal controls using standardized low-resolution electromagnetic tomography (sLORETA) [5] combined with normative independent component analysis techniques. They found low-frequency power excess (2–6 Hz) in the medial frontal cortex with sLORETA and increased low-frequency power in a component reflecting the activity of subgenual anterior cingulate and adjacent limbic structures with normative independent component analysis. These findings have been interpreted as evidence for the medial frontal hyperactivation in OCD. In addition, there are several significant findings that implicate the anterior cingulate [6–8], using LORETA. Neuroimaging studies using functional magnetic resonance (fMRI) have detected hyperactivity of the performance-monitoring system in OCD, consistent with hyperactivation of the anterior cingulate cortex and the medial frontal cortex [9, 10]. It has been hypothesized that the hyperactive performance-monitoring system generates a feeling that something is unreasonable or irrational, triggering compulsive behavior, thus providing a possible explanation of how brain abnormalities translate into the clinical symptoms of OCD [11]. This leads to a question of great interest: can we detect hyperactivation of the performance-monitoring system under symptom provocation?

Symptom provocation studies using EEG recordings are very scarce, as compared to symptom provocation studies using conventional neuroimaging techniques. To the best of our knowledge, only a preliminary study was reported [12] using quantitative EEG analysis with symptom provocation in OCD patients. They confirmed a significant change of alpha power distribution from anterior to posterior not by imaginative symptom exposure but by live symptom exposure. But unfortunately, EEG data in this study were seriously contaminated with muscle artifacts due to the live exposure procedure, and furthermore, the data from just a small number of electrodes were available for quantitative analysis.

Scalp electric potential fields from EEG recordings reflect the dynamics of the functional state of the brain. The determination of the brain states and their time sequencing are essential for characterizing and understanding both normal and pathological function. This is of particular interest when studying behavioral disorders, which are not due to localized brain lesions but are related to the deviant use of brain resources. It has been systematically observed that by viewing multichannel EEG recordings as sequences of instantaneous scalp electric potential distributions (i.e., maps) instead of wave shapes, certain map configurations (irrespective of amplitude and polarity) persist during extended epochs (time segments) and that they change rapidly to new configurations that are stable again for given time periods [13]. These time segments of stable map configurations presumably reflect the different steps or modes or contents of information processing, i.e. the functional microstates of the brain [13–15]. Changes in the spatial distribution of the signal correspond to segment changes and reflect changes of the functional state.

The EEG microstates during rest constitute the electrophysiological counterpart of the now popular metabolic resting state networks. Indeed, as reviewed by Lehmann [14], 2 recent studies [16, 17] have demonstrated the relation between the 2 approaches.

A number of interesting microstate analysis findings have been reported in the field of psychiatric or neurological disorders, such as in schizophrenia [18–22], depression [23], and dementia [24]. However, to the best of our knowledge, there are no previous EEG microstate studies in OCD patients.

In this EEG study, we compared an imaginative exposure condition with the resting state condition, both within and between 2 groups of subjects: OCD patients and normal control subjects. We modeled the EEGs under the assumption that both groups use the same brain resources, characterized by 4 microstate scalp maps (i.e., resting state networks) common to OCD and normal control subjects. We tested the hypotheses that the microstate dynamics given by features such as durations, frequencies of occurrence, and Markov transition rates, would reflect differences related to the pathological information processing in OCD, particularly localized to frontal regions including the anterior cingulate cortex, which plays a major role in conflict monitoring.

Material and Methods

Subjects

The study protocol was approved by the institutional review board of Kansai Medical University, and written informed consent was obtained from all participants. Nine OCD outpatients (3 men and 6 women; average age: 27.1 ± 9.8 years) and 9 healthy controls (4 men and 5 women; average age: 25.6 ± 5.8 years) participated in this study. The OCD patients were treated at the clinic of psychiatry of Kansai Medical University Takii Hospital. All patients had received a diagnosis of OCD based on the Diagnostic and Statistical Manual of Mental Disorders, fourth edition (DSM-IV) [25]. We excluded patients who: had substantial medical illness or neurological (e.g., Tourette syndrome, Huntington disease, and Parkinson disease), pulmonary, cardiac, renal, hepatic, endocrine, or metabolic disorders; had DSM-IV-defined dementia, delirium, schizophrenia, schizoaffective disorder, delusional disorder, brief reactive psychosis, or psychotic disorders not otherwise specified; had DSM-IV-defined mental retardation; had lacunar infarcts; were currently or previously dependent on or abusers of DSM-IV-defined alcoholic or psychoactive substances; and/or were pregnant [26]. For the estimation of obsessive and compulsive symptoms, the Japanese version of the Yale Brown Obsessive Compulsive Scale was applied; its average score was 25.0 ± 8.5. Six of 9 patients were already medicated at the time of the EEG recording. Three patients were taking paroxetine hydrochloride only, 1 patient a combination of paroxetine hydrochloride and benzodiazepines, and 1 patient a combination of fluvoxamine hydrochloride and benzodiazepines, 1 patient a combination of paroxetine hydrochloride, fluvoxamine maleate and maprotiline hydrochloride.

Recordings

All subjects were recorded while seated in a quiet environment with dimmed light. Electrodes were attached to the scalp with conductive paste at the following positions of the International 10-20 System: Fp1, Fp2, F7, F3, Fz, F4, F8, T3, C3, Cz, C4, T4, T5, P3, Pz, P4, T6, O1, and O2, with linked earlobes used as reference. Electrode impedances were kept below 10 kΩ. The EEG was band-pass filtered from 0.3 to 30 Hz, amplified, digitized (200 Hz), and digitally stored using an EEG Nihon Koden system (Nihon Koden, Tokyo, Japan).

Experimental Conditions

Eyes closed recordings for the OCD subjects were performed under 4 sequential conditions:

C1, initial rest: resting, awake, alert condition

C2, clean control: subjects gently held a clean towel in their hands

C3, imaginative exposure condition: subjects were instructed to imagine that the towel in their hands was contaminated with the material that invoked the feeling of disgust

C4, final rest: same as C1, i.e. resting, awake, alert condition

The healthy control group was recorded under the baseline condition C1 only, denoted as "resting state".

The extent of obsession in the OCD patients and the obsession-like anxiety of the healthy controls associated with the feeling of disgust as induced by the stimulus were measured by means of a visual analog scale (VAS) after each condition. The VAS score was compared using paired comparisons between conditions, for each group (OCD or control).

The conditions lasted 5 min each. For each EEG recording condition, 20 artifact-free epochs of 2-s duration each were randomly selected by visual inspection for analysis, excluding eye movements, blinks, and signs of drowsiness.

Prior to microstate analysis, the selected data were recomputed against average reference and band-pass filtered to 2–20 Hz [21, 27].

Analysis

Microstate scalp electric potential maps were estimated from the total EEG recordings, consisting of 256 scalp maps for each 2-s EEG epoch, with 20 epochs per subject (9 OCD patients and 9 normal controls), under the 4 conditions previously described for the OCD group, and under the baseline resting state for the healthy control group.

An intuitive and comprehensive description of microstate theory was provided in the "Introduction" section. As explained there, EEG microstates are scalp map configurations that persist during time segments of finite duration and that change rapidly into new configurations that are again stable for given time periods [13]. This can be expressed mathematically as:

$$\Phi_t = a_{kt}\Gamma_k$$

where $\Phi_t \in \mathbb{R}^{N_E \times 1}$ denotes the time varying ("t") average reference map of scalp electric potentials at N_E electrodes; $\Gamma_k \in \mathbb{R}^{N_E \times 1}$ denotes the k-th normalized microstate map; and the coefficients a_{kt} denote the amplitudes. The index (subscript) "k" takes integer values in the range $1 \ldots N_M$, where N_M denotes the number of different microstate maps. Note that the actual microstate map "k" is a function of time, and can be expressed as:

$$k = L(t).$$

This model can be optimally estimated by means of the algorithm derived in Pascual-Marqui et al. [28].

The actual number of microstate maps was determined by the minimum cross-validation error criterion, applied to the microstate model [28]. This criterion selects the number of microstates that best explains the actual recordings in a predictive way. Overfitting is avoided because of the predictive nature of cross-validation, which is implicitly based on the concept of "leave one out".

Once the microstate maps common to all recordings were estimated, the microstate parameters were computed for each subject and condition. The essential parameters for each microstate map were:

1. Percent of explained global field power by each microstate, relative to the actual total global field power, which is always below 100% (%GFP)
2. Percent of time (contribution) spent in each microstate (%T)
3. Frequency of occurrence (FO), consisting of the average number of occurrences of microstate segments (independent of the duration of each segment) per second

In addition, the dynamic transitions between microstates were characterized by means of the Markov transition rate matrix [29], which provides information on the "syntax" of brain state [15]. The element in the i-th row and j-th column corresponds to the average number of transitions (i.e., jumps) per second from microstate "i" to microstate "j". The diagonal element in the i-th row and column is equal to the negative value of the sum of the nondiagonal elements in the i-th row, due to the conservation principle of transitions. Note that large negative values for a diagonal element cor-

Table 1. Average microstate (MSt) parameters for the normal control group

	MSt A	MSt B	MSt C	MSt D
%GFP	7.33	8.36	14.04	32.18
%T	15.65	17.83	24.95	41.57
FO	4.63	4.83	5.93	6.92
Markov rate A	–14.16	3.37	4.58	6.21
Markov rate B	2.79	–12.95	4.30	5.86
Markov rate C	3.00	3.12	–11.28	5.17
Markov rate D	2.37	2.41	3.20	–7.98

%GFP, percentage of explained global field power relative to the total EEG GFP; %T, percentage of time spent in each microstate; FO, frequency of occurrence (average number of occurrences per second); Markov transition rates in units of number of microstate transitions (row to column) per second.

Table 2. Average microstate (MSt) parameters for the OCD group

	MSt A	MSt B	MSt C	MSt D
%GFP	8.43	7.33	16.01	23.35
%T	20.14	18.24	29.45	32.16
FO	5.93	5.53	6.96	6.58
Markov rate A	–14.14	3.76	5.65	4.72
Markov rate B	4.20	–14.62	5.38	5.05
Markov rate C	3.70	3.29	–11.32	4.33
Markov rate D	3.10	2.88	3.80	–9.78

%GFP, percentage of explained global field power relative to the total EEG GFP; %T, percentage of time spent in each microstate; FO, frequency of occurrence (average number of occurrences per second); Markov transition rates in units of number of microstate transitions (row to column) per second.

respond to a larger number of transitions that escape from the corresponding microstate, indicating more instability of the microstate. Equivalently, small negative values for a diagonal element correspond to a smaller number of transitions that escape from the corresponding microstate, indicating more stability of the microstate.

Statistical comparisons of two types were performed:

1. Paired comparisons between conditions for the OCD group
2. Nonpaired comparisons between groups, for each condition in the OCD group as compared to baseline resting state EEG for the healthy control group

All parameters (%GFP, %T, FO, and the transition rates) were statistically compared by appropriate *t* tests, and when relevant, effect size [30] is also reported.

In addition to the microstate parameters, the cortical distribution of electric neuronal activity for each microstate is calculated by means of sLORETA [5]. The methodology for this straightforward analysis has been previously described [31]. It should be noted that this new approach makes a one-to-one correspondence between each classical microstate scalp map and its corresponding cortical generator distribution.

Results

The feeling of disgust as assessed by the VAS was significantly increased in the imaginative exposure condition (C3) as compared to the clean control condition (C2) (OCD: $p = 0.016$, control: $p = 0.006$), which then decreased after the exposure (C4) in OCD patients (OCD: $p = 0.003$).

Four microstate maps were found to be adequate for the entire data consisting of 2 groups (9 OCD patients and 9 normal control subjects) under 4 recording conditions (initial rest, clean control condition while holding towel in hands, imaginative exposure to contaminated towel, and final rest) for OCD, and baseline resting state for healthy controls. This number of microstates corresponded to the minimum cross-validation error for model selection [28]. This result is in agreement with many previous resting state EEG studies; 4 microstate scalp maps have been found to adequately represent the recordings [15, 21, 24, 27].

Tables 1 and 2 show the average values for the microstate parameters, for the normal control and control group, respectively.

Figure 1 shows the microstate scalp maps and their corresponding electric neuronal generator distribution on the cortex, as obtained with sLORETA [5]. The 4 microstate scalp maps are labeled with uppercase letters "A", "B", "C", and "D", which correspond to those reported in e.g. Koenig et al. [32]. The sLORETA images corresponding to each microstate scalp map were z-transformed and are displayed with a color scale that emphasizes z-values higher than 3. This method is the same as the one used for the identification and display of functional resting state networks, see e.g. Agcaoglu et al. and others [33–36]. Table 3 lists the neuroanatomical regions that are maximally active for each microstate.

Paired Comparisons between Conditions in the OCD Group

All microstate parameters were compared between conditions in the OCD group. The effect sizes and *t* values for significant differences for the tests at $p < 0.05$ (uncorrected) were observed only for C3 (imaginative exposure) compared to C2 (clean control), as shown in Table 4. The %GFP and the Markov transition rate of remaining in

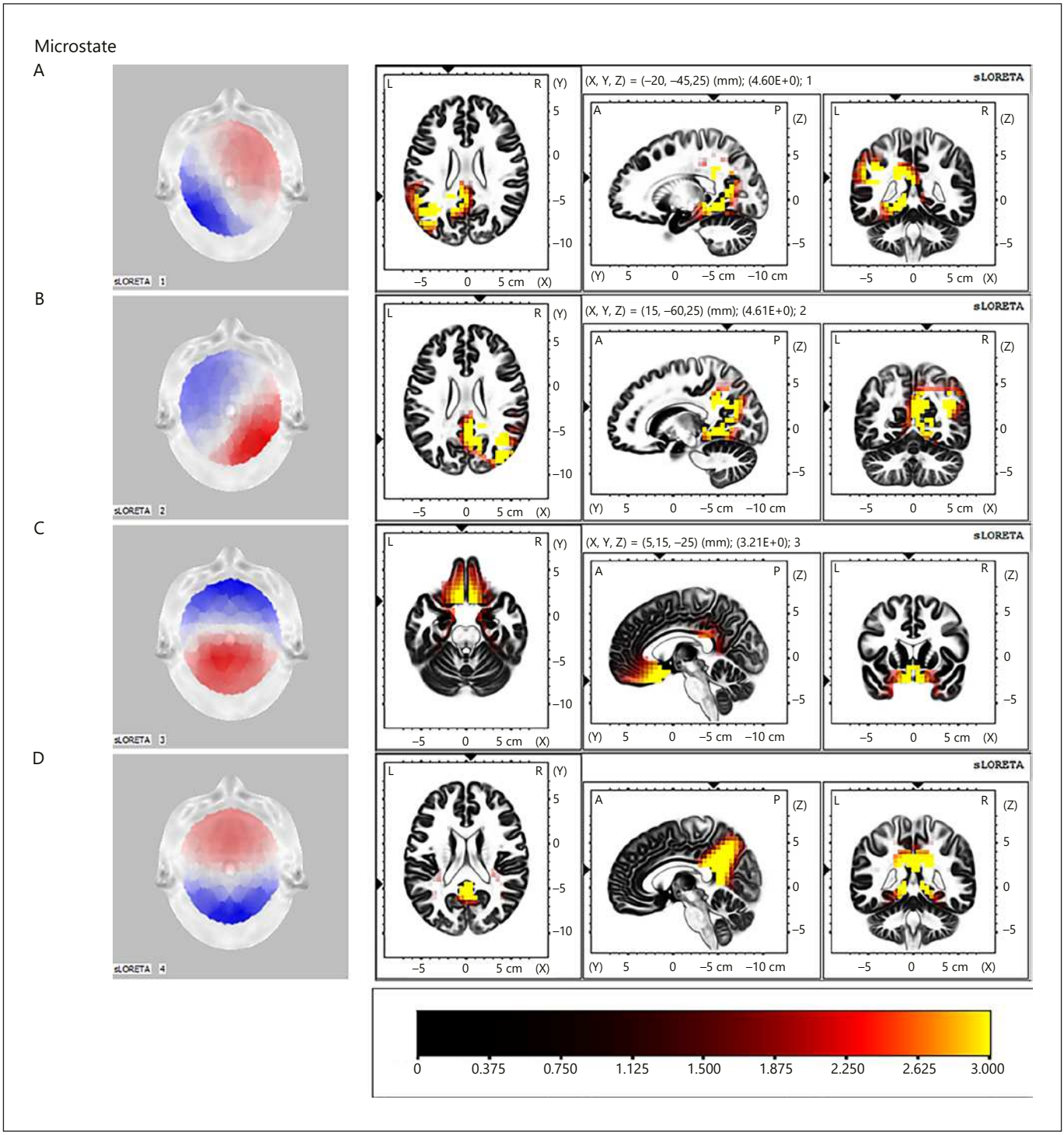

Fig. 1. Rows 1–4 correspond to the respective microstates, with the leftmost column corresponding to the classic letter designation A–D. The second column displays the scalp electric potential map, with positive and negative values color coded as red and blue, respectively. The third to fifth columns display the z-transformed electric neuronal generator distribution on the cortex, corresponding to axial, sagittal, and coronal views, respectively. The orthogonal slices are shown at the maximum activity. L, left; R, right; A, anterior; P, posterior. Color scale for z-transformed cortical electric neuronal activity, emphasizing z-values higher than 3.

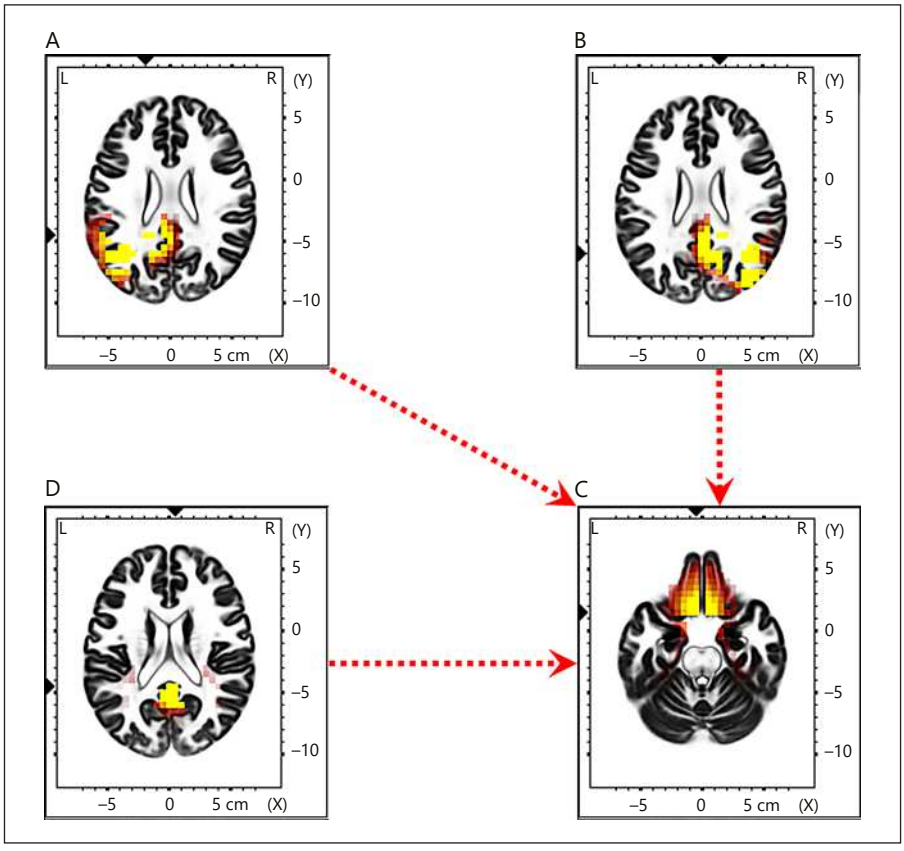

Fig. 2. Significant differences for Markov transitions in OCD, for C3 (imaginative exposure) compared to C2 (clean control). Dashed red arrows converging on microstate "C" indicate a stable attractor state with lower escape transitions during imaginative exposure. In other words, in the OCD group, during imaginative exposure (as compared to rest), microstates "A", "B", and "D" are unstable and jump into microstate "C". Note that the microstates are now shown in the form of the computed cortical generators based on sLORETA, rather than with traditional scalp maps.

Table 3. Cortical localizations of electric neuronal activity maxima for each microstate

Microstate	Brain regions
A	Left parietal + posterior cingulate
B	Right parietal + posterior cingulate
C	Medial frontal + anterior cingulate
D	Posterior cingulate + precuneus

Table 4. Observed significant differences (uncorrected $p < 0.05$) of microstate (MSt) parameters, between conditions, for the OCD group

Group	Contrast	Parameter	*t* value	Effect size
OCD	C3-C2	%GFP MSt C	2.04	0.72
OCD	C3-C2	Markov rate MSt C to MSt C	2.02	0.71

%GFP, percentage of explained global field power relative to the total EEG GFP.

microstate "C" were the only parameters displaying a significant difference, with a moderate to large effect size [30].

The positive *t* value for the self Markov transition rate from microstate C to microstate C indicates that it is a stable "attractor state" during imaginative exposure as compared to the clean control condition. In other words, in the OCD group, during imaginative exposure (as compared to rest), microstates "A", "B", and "D" are unstable and jump into microstate "C". This result is schematically illustrated in Figure 2, which shows in the form of arrows microstate "C" as an attractor. It is noted that in Figure 2, rather than illustrating microstates by traditional scalp maps, they are now shown in the form of the computed cortical generators based on sLORETA.

Comparisons between Groups (OCD and Healthy Control)

Each microstate parameter for each condition (C1, C2, C3, and C4) in the OCD group was compared to the baseline resting state parameters of the healthy control group.

Table 5. Effect size (Cohen's *d*) values for all microstate (MSt) parameters, for "OCD in condition 1 (initial rest)" compared to "healthy control in baseline resting state (CTRL)"

OCD1-CTRL	MSt A	MSt B	MSt C	MSt D
%GFP	0.55	–0.38	–0.31	–0.71
%T	0.68	0.04	0.13	–0.55
FO	1.10	1.04	0.96	0.37
Markov rate A	–0.41	0.09	1.16	–0.34
Markov rate B	0.65	–0.56	0.37	0.08
Markov rate C	1.01	0.41	–0.57	–0.16
Markov rate D	1.08	0.78	0.57	–0.99

Positive values highlighted in red indicate significantly higher OCD values with uncorrected $p < 0.05$ and with very large effect size $d > 0.95$, whereas negative values highlighted in green indicate significantly lower OCD values with uncorrected $p < 0.05$ and with very large effect size $|d| > 0.95$. %GFP, percentage of explained global field power; %T, percentage of time spent in each microstate; FO, frequency of occurrence (average number of occurrences per second); Markov transition rates (row to column).

Table 6. Effect size (Cohen's *d*) values for all microstate (MSt) parameters, for "OCD in condition 2 (clean control)" compared to "healthy control in baseline resting state (CTRL)"

OCD2-CTRL	MSt A	MSt B	MSt C	MSt D
%GFP	0.24	–0.54	0.23	–0.64
%T	0.54	–0.12	0.34	–0.57
FO	1.21	0.72	0.90	0.13
Markov rate A	–0.89	0.15	1.07	–0.16
Markov rate B	0.77	–0.57	0.26	–0.07
Markov rate C	1.02	0.28	–0.43	–0.21
Markov rate D	0.93	0.84	0.71	–1.07

Positive values highlighted in red indicate significantly higher OCD values with uncorrected $p < 0.05$ and with very large effect size $d > 0.95$, whereas negative values highlighted in green indicate significantly lower OCD values with uncorrected $p < 0.05$ and with very large effect size $|d| > 0.95$. %GFP, percentage of explained global field power; %T, percentage of time spent in each microstate; FO, frequency of occurrence (average number of occurrences per second); Markov transition rates (row to column).

The effect sizes (Cohen's *d*) for all tests are reported in Tables 5–7, corresponding to the contrasts for [(OCD in C1) – (CTRL resting state)], [(OCD in C2) – (CTRL resting state)], and [(OCD on C3) – (CTRL resting state)], respectively. Positive values highlighted in red indicate significantly higher OCD values with uncorrected $p < 0.05$ and with very large effect size $d > 0.95$, whereas negative values highlighted in green indicate significantly lower OCD values with uncorrected $p < 0.05$ and with very large effect size $|d| > 0.95$. The contrast [(OCD in C4) – (control resting state)] did not yield any significant result.

In summary, significant differences were found only for the frequency of occurrence parameter and for the Markov transition rates. With respect to the frequency of occurrence, it was higher for OCD in C1 for microstates A-B-C, and in C2 for microstate A. With respect to the Markov transition rates, the common trait for all significant OCD conditions compared to resting state control consists of significant transition rates from microstate "A" to "C", together with high instability of microstate "D", as shown in Figure 3.

Table 7. Effect size (Cohen's *d*) values for all microstate (MSt) parameters, for "OCD in condition 3 (imaginative exposure)" compared to "healthy control in baseline resting state (CTRL)"

OCD3-CTRL	MSt A	MSt B	MSt C	MSt D
%GFP	0.16	–0.56	0.50	–0.68
%T	0.47	–0.24	0.54	–0.72
FO	0.79	0.30	0.89	0.05
Markov rate A	–0.31	0.08	0.96	–0.34
Markov rate B	0.48	–0.45	0.47	–0.12
Markov rate C	0.55	–0.21	0.08	–0.49
Markov rate D	0.96	0.53	0.65	–1.01

Positive values highlighted in red indicate significantly higher OCD values with uncorrected $p < 0.05$ and with very large effect size $d > 0.95$, whereas negative values highlighted in green indicate significantly lower OCD values with uncorrected $p < 0.05$ and with very large effect size $|d| > 0.95$. %GFP, percentage of explained global field power; %T, percentage of time spent in each microstate; FO, frequency of occurrence (average number of occurrences per second); Markov transition rates (row to column).

Discussion

We applied imaginative symptom exposure to induce the feeling of disgust in this study, rather than using live symptom exposure. The feeling of disgust was significant during imaginative exposure, which then quickly decreased after its termination. This symptom provocation procedure was partly based on reports from a previous study [37]. The stimulation was well tolerated by all subjects, thus being compliant with ethical considerations.

A very basic first result corresponds to the actual microstates obtained in this study, as shown in Figure 1. The 4 microstates have cortical electric neuronal generators

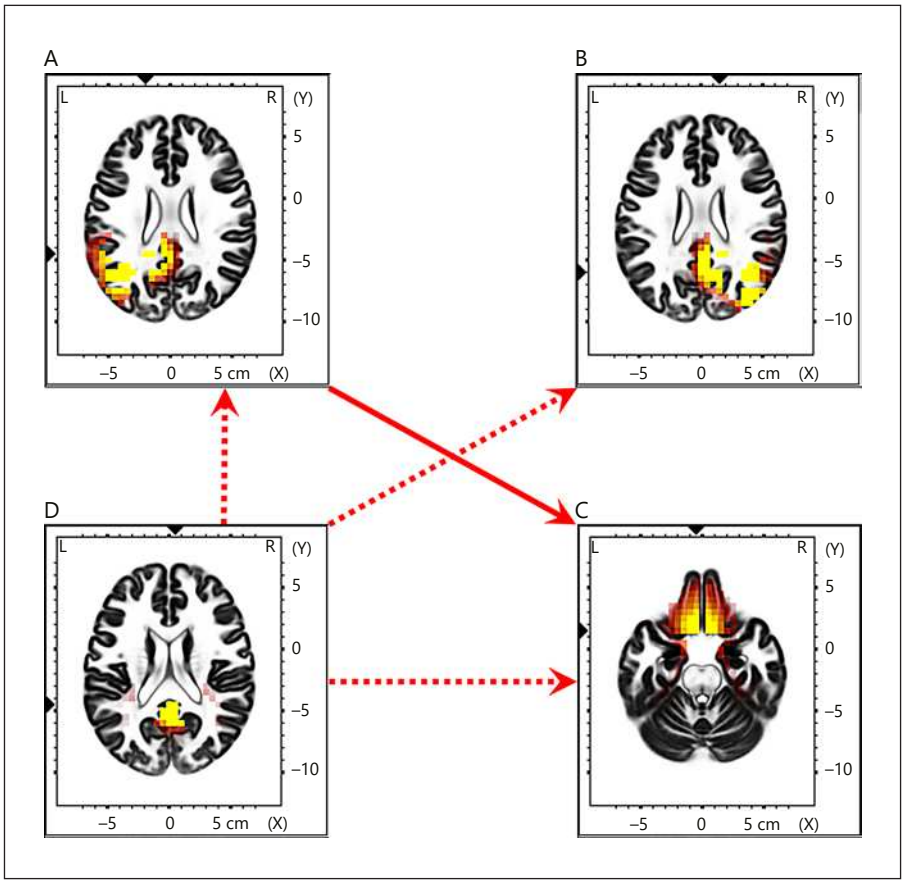

Fig. 3. Common trait for OCD conditions C1 (initial rest), C2 (clean control), and C3 (imaginative exposure) compared to resting state control. A significantly higher transition rate for OCD, from microstate "A" to "C", is indicated with a solid red arrow. Significant instability for OCD microstate "D", based on its high escape transition rate, is indicated with dashed red arrows diverging from microstate "D".

that basically correspond to the main 4 brain regions that have been implicated in the metabolic default mode network (see, for instance, Raichle and Snyder [38]), as indicated in Table 3. These same microstate scalp maps and cortical generators were previously obtained in the analysis of an independent EEG study for 109 subjects recorded in the baseline eyes closed resting state condition [31]. There it was shown that all microstates have common posterior cingulate generators, while 3 microstates additionally include activity in the left parietal, right parietal, and anterior cingulate cortices. These results are in correspondence with the notion that EEG microstates consist of a spatially fragmented version of the metabolically (PET/fMRI) computed default mode network, supporting the notion that these 4 regions activate sequentially at high time resolution, and that slow metabolic imaging corresponds to a very low time resolution version.

A qualitative comparison of the microstate scalp maps "A", "B", "C", and "D" obtained in this study (shown in Fig. 1) with those reported in other EEG studies (see e.g. Koenig et al. [32]) shows excellent qualitative agreement.

Comparisons of microstate parameters between condition, within the OCD group, revealed significant differences only for condition 3 (imaginative exposure) compared to condition 2 (clean exposure). Microstate "C" (anterior cingulate) accounted for higher global field power during imaginative exposure. From a dynamics point of view, our results show that microstate "C" (anterior cingulate) is a preferred state (i.e., an attractor state) during imaginative exposure, with significantly low escape transitions.

Between-group comparisons, between each OCD condition and the healthy control group in baseline resting state, showed that the frequencies of occurrence were higher in some OCD conditions (Tables 5–7), for microstates "A" (left inferior parietal), "B" (right inferior parietal), and "C" (anterior cingulate).

From a dynamics point of view, there are 2 main results which are a common trait to OCD conditions C1, C2, and C3 compared to baseline resting state control: firstly, significant transition rates from microstate "A" (left inferior parietal) to "C" (anterior cingulate) in OCD;

secondly, significant instability with high escape rates microstate "D" (posterior cingulate) in OCD.

In summary, the dynamic transitions between microstates differ significantly between OCD and normal controls, with microstate "D" (posterior cingulate) being a "repulsor" state for OCD, while microstate "C" (anterior cingulate) is an "attractor" state for OCD. A possible interpretation, based on the different cortical locations, is consistent with the notion that OCD patients make more use of part of the frontal control network [9] including the anterior cingulate, whereas the normal controls perform the imaginative act using significantly more the visual cortex, but without excessive control.

It is worth pointing out another important observation with respect to the transitions between microstates. The OCD patients have a connectivity pattern with significant transitions from posterior to anterior brain regions (microstate "A" to "C", i.e. left inferior parietal to anterior cingulate regions). This result, which agrees with the previously explained view, might correspond to stronger engagement of frontal control networks in OCD, which seems plausible due to the thought disorder of OCD, with excessive thought processing related to the object of obsession. In addition, the observed abnormal transition rates between posterior and frontal brain regions in the OCD group might very well have its anatomical basis in the reduced white matter connectivity observed in a DTI study by Garibotto et al. [39]. Moreover, the transitions from anterior to posterior cortical activation in OCD patients induced by imaginative exposure partly corresponded to the previous symptom provocation study using quantitative EEG by Simpson et al. [12].

This study has a number of limitations. Primarily, the number of subjects is small. Furthermore, 6 of 9 OCD patients were already medicated with more than one drug, including the concomitant use of antidepressants and benzodiazepine. This, unfortunately, is a problem shared by the majority of OCD research papers, as reviewed in Posner et al. [40]. However, the aim of this study was to investigate the changes of brain electric field induced by symptom provocation in OCD patients in comparison to healthy controls. Therefore, the heterogeneity of the OCD patients in this study can be considered to be a realistic factor.

Despite these problems, the significance of this study clearly outweighs the limitations, where it is shown that noninvasive and low-cost EEG recordings can be used as an important low-spatial resolution neuroimaging technique that in addition, reveals high time resolution dynamic brain processes. In future studies, higher density EEG recordings should be used.

Acknowledgments

M. Yoshimura was supported for this study by a grant from SENSHIN Medical Research Foundation during his stay at the University Hospital of Psychiatry, Bern, and partially supported by the Center of Innovation (COI) Program of the Japan Science and Technology Agency (JST), Japan. The funders had no role in the study design, data collection and analysis, decision to publish or preparation of the manuscript. The authors appreciate the enthusiastic participation of a group of students from the University of Bern.

Disclosure Statement

The authors declare no conflicts of interest.

References

1 American Psychiatric Association: Diagnostic and Statistical Manual of Mental Disorders, ed 5 (DSM-5). Arlington, American Psychiatric Publishing, 2013.
2 Kaplan HI, Sadock BJ: Kaplan and Sadock's Synopsis of Psychiatry: Behavioral Sciences/Clinical Psychiatry. Baltimore, Lippincott Williams & Wilkins, 2003.
3 Saxena S, Rauch SL: Functional neuroimaging and the neuroanatomy of obsessive-compulsive disorder. Psychiatr Clin North Am 2000;23:563–586.
4 Koprivova J, Congedo M, Horacek J, Prasko J, Raszka M, Brunovsky M, Kohutova B, Hoschl C: EEG source analysis in obsessive-compulsive disorder. Clin Neurophysiol 2011;122:1735–1743.
5 Pascual-Marqui RD: Standardized low-resolution brain electromagnetic tomography (sLORETA): technical details. Methods Find Exp Clin Pharmacol 2002;24(suppl D):5–12.
6 Fontenelle LF, Mendlowicz MV, Ribeiro P, Piedade RA, Versiani M: Low-resolution electromagnetic tomography and treatment response in obsessive-compulsive disorder. Int J Neuropsychopharmacol 2006;9:89–94.
7 Sherlin L, Congedo M: Obsessive-compulsive dimension localized using low-resolution brain electromagnetic tomography (LORETA). Neurosci Lett 2005;387:72–74.
8 Velikova S, Locatelli M, Insacco C, Smeraldi E, Comi G, Leocani L: Dysfunctional brain circuitry in obsessive-compulsive disorder: source and coherence analysis of EEG rhythms. Neuroimage 2010;49:977–983.
9 Fitzgerald KD, Welsh RC, Gehring WJ, Abelson JL, Himle JA, Liberzon I, Taylor SF: Error-related hyperactivity of the anterior cingulate cortex in obsessive-compulsive disorder. Biol Psychiatry 2005;57:287–294.
10 Ursu S, Stenger VA, Shear MK, Jones MR, Carter CS: Overactive action monitoring in obsessive-compulsive disorder: evidence from functional magnetic resonance imaging. Psychol Sci 2003;14:347–353.

11 Maltby N, Tolin DF, Worhunsky P, O'Keefe TM, Kiehl KA: Dysfunctional action monitoring hyperactivates frontal-striatal circuits in obsessive-compulsive disorder: an event-related fMRI study. Neuroimage 2005;24:495–503.
12 Simpson HB, Tenke CE, Towey JB, Liebowitz MR, Bruder GE: Symptom provocation alters behavioral ratings and brain electrical activity in obsessive-compulsive disorder: a preliminary study. Psychiatry Res 2000;95:149–155.
13 Lehmann D, Ozaki H, Pal I: EEG alpha map series: brain micro-states by space-oriented adaptive segmentation. Electroencephalogr Clin Neurophysiol 1987;67:271–288.
14 Lehmann D: Multimodal analysis of resting state cortical activity: what does fMRI add to our knowledge of microstates in resting state EEG activity? Commentary to the papers by Britz et al. and Musso et al. in the current issue of NeuroImage. Neuroimage 2010;52:1173–1174.
15 Lehmann D, Pascual-Marqui RD, Michel C: EEG microstates. Scholarpedia 2009;4:7632.
16 Britz J, Van de Ville D, Michel CM: BOLD correlates of EEG topography reveal rapid resting-state network dynamics. Neuroimage 2010;52:1162–1170.
17 Musso F, Brinkmeyer J, Mobascher A, Warbrick T, Winterer G: Spontaneous brain activity and EEG microstates. A novel EEG/fMRI analysis approach to explore resting-state networks. Neuroimage 2010;52:1149–1161.
18 Kikuchi M, Koenig T, Wada Y, Higashima M, Koshino Y, Strik W, Dierks T: Native EEG and treatment effects in neuroleptic-naive schizophrenic patients: time and frequency domain approaches. Schizophr Res 2007;97:163–172.
19 Irisawa S, Isotani T, Yagyu T, Morita S, Nishida K, Yamada K, Yoshimura M, Okugawa G, Nobuhara K, Kinoshita T: Increased omega complexity and decreased microstate duration in nonmedicated schizophrenic patients. Neuropsychobiology 2006;54:134–139.
20 Strelets V, Faber PL, Golikova J, Novototsky-Vlasov V, Koenig T, Gianotti LR, Gruzelier JH, Lermann D: Chronic schizophrenics with positive symptomatology have shortened EEG microstate durations. Clin Neurophysiol 2003;114:2043–2051.
21 Koenig T, Lehmann D, Merlo MC, Kochi K, Hell D, Koukkou M: A deviant EEG brain microstate in acute, neuroleptic-naive schizophrenics at rest. Eur Arch Psychiatry Clin Neurosci 1999;249:205–211.
22 Rieger K, Hernandez LD, Baenninger A, Koenig T: 15 years of microstate research in schizophrenia – where are we? A meta-analysis. Front Psychiatry 2016;7:22.
23 Strik WK, Dierks T, Becker T, Lermann D: Larger topographical variance and decreased duration of brain electric microstates in depression. J Neural Transm Gen Sect 1995;99:213–222.
24 Nishida K, Morishima Y, Yoshimura M, Isotani T, Irisawa S, Jann K, Dierks T, Strik W, Kinoshita T, Koenig T: EEG microstates associated with salience and frontoparietal networks in frontotemporal dementia, schizophrenia and Alzheimer's disease. Clin Neurophysiol 2013;124:1106–1114.
25 American Psychiatric Association: Diagnostic and Statistical Manual of Mental Disorders, ed 4 (DSM-IV). Arlington, American Psychiatric Publishing, 2000.
26 Saito Y, Nobuhara K, Okugawa G, Takase K, Sugimoto T, Horiuchi M, Ueno C, Maehara M, Omura N, Kurokawa H, Ikeda K, Tanigawa N, Sawada S, Kinoshita T: Corpus callosum in patients with obsessive-compulsive disorder: diffusion-tensor imaging study. Radiology 2008;246:536–542.
27 Kikuchi M, Koenig T, Munesue T, Hanaoka A, Strik W, Dierks T, Koshino Y, Minabe Y: EEG microstate analysis in drug-naive patients with panic disorder. PLoS One 2011;6:e22912.
28 Pascual-Marqui RD, Michel CM, Lehmann D: Segmentation of brain electrical activity into microstates: model estimation and validation. IEEE Trans Biomed Eng 1995;42:658–665.
29 Basawa IV, Rao BP: Statistical Inference for Stochastic Processes. London, Academic Press, 1980.
30 Cohen J: Statistical Power Analysis for the Behavioral Sciences, ed 2. Hillsdale, Lawrence Erlbaum Associates, 1988.
31 Pascual-Marqui RD, Lehmann D, Faber P, Milz P, Kochi K, Yoshimura M, Nishida K, Isotani T, Kinoshita T: The resting microstate networks (RMN): cortical distributions, dynamics, and frequency specific information flow. 2014, November 7. arXiv preprint arXiv:1411.1949. http://arxiv.org/abs/1411.1949.
32 Koenig T, Prichep L, Lehmann D, Sosa PV, Braeker E, Kleinlogel H, Isenhart R, John ER: Millisecond by millisecond, year by year: normative EEG microstates and developmental stages. Neuroimage 2002;16:41–48.
33 Agcaoglu O, Miller R, Mayer A, Hugdahl K, Calhorn V: Lateralization of resting state networks and relationship to age and gender. Neuroimage 2015;104:310–325.
34 Aoki Y, Ishii R, Pascual-Marqui RD, Canuet L, Ikeda S, Hata M, Imajo K, Matsuzaki H, Musha T, Asada T, Iwase M, Takeda M: Detection of EEG-resting state networks by LORETA-ICA method. Front Hum Neurosci 2015;9:31.
35 Calhoun VD, Kiehl KA, Liddle PF, Pearlson GD: Aberrant localization of synchronous hemodynamic activity in auditory cortex reliably characterizes schizophrenia. Biol Psychiatry 2004;55:842–849.
36 McKeown MJ, Makeig S, Brown GG, Jung T-P, Kindermann SS, Bell AJ, Sejnowski TJ: Analysis of fMRI data by blind separation into independent spatial components. Hum Brain Mapp 1998;6:160–188.
37 Adler CM, Mcdonough-Ryan P, Sax KW, Holland SK, Arndt S, Strakowski SM: fMRI of neuronal activation with symptom provocation in unmedicated patients with obsessive compulsive disorder. J Psychiatr Res 2000;34:317–324.
38 Raichle ME, Snyder AZ: A default mode of brain function: a brief history of an evolving idea. Neuroimage 2007;37:1083–1090; discussion 1097–1099.
39 Garibotto V, Scifo P, Gorini A, Alonso CR, Brambati S, Bellodi L, Perani D: Disorganization of anatomical connectivity in obsessive compulsive disorder: a multi-parameter diffusion tensor imaging study in a subpopulation of patients. Neurobiol Dis 2010;37:468–476.
40 Posner J, Marsh R, Maia TV, Peterson BS, Gruber A, Simpson HB: Reduced functional connectivity within the limbic cortico-striato-thalamo-cortical loop in unmedicated adults with obsessive-compulsive disorder. Hum Brain Mapp 2014;35:2852–2860.